Crystallization of [Ga]-MFI under atmospheric pressure

Jinu Park [a], Sang-Bum Kim [a], Jae-Mok Ha [b], Hong-Soo Park [a] and Hyun-Sik Hahm [a,*]

[a] *Department of Chemical Engineering, Myongji University, Yongin 449-728, South Korea*
E-mail: hahm@mju.ac.kr
[b] *Agency for Technology and Standards, Kwacheon 427-716, South Korea*

Received 22 March 2001; accepted 31 May 2001

The crystallization of [Ga]-MFI was investigated as a function of synthesis time under atmospheric pressure. The molar composition of the reactants was $100SiO_2$–Ga_2O_3–$11Na_2O$–11TPABr–$3500H_2O$. The crystallinity of [Ga]-MFI was examined using several analytical instruments, such as XRD, XPS, XRF, FT-IR, solid state MAS-NMR, and DTG/DTA. [Ga]-MFI was successfully synthesized under atmospheric pressure at 97 °C in 72 h. It was found that the nucleation of [Ga]-MFI took quite a long time, but the crystallization took place very fast. It is supposed that the nucleation is the rate-controlling step in [Ga]-MFI synthesis under atmospheric pressure. Consequently, if the induction period of the nucleation can be shortened, it would be possible to synthesize [Ga]-MFI commercially under atmospheric pressure.

KEY WORDS: zeolite; [Ga]-MFI; gallosilicate; atmospheric pressure synthesis; ^{71}Ga-MAS-NMR

1. Introduction

[Ga]-MFI is a zeolite, which is prepared by the substitution of Ga for Al in the framework of ZSM-5. [Ga]-MFI shows high activity and selectivity in the aromatization of lower alkanes, which is a process of great commercial importance [1–4]. There are several reported methods to incorporate Ga into the MFI zeolite: ion exchange [5,6], impregnation [7,8], physical mixing of Ga_2O_3 with MFI zeolite [9,10], and partial or full substitution of Ga for Al of the MFI zeolite [11–20]. Recently, the last method has drawn interest because of the even distribution of gallium, which exhibits higher dehydrogenation activity. Until now, [Ga]-MFIs have been synthesized using autoclaves under an autogenous pressure above 150 °C [21–23].

In this study, the synthesis of [Ga]-MFI type zeolite was conducted using a Teflon reactor under atmospheric pressure, and the crystallization of [Ga]-MFI was also investigated.

2. Experimental

2.1. Synthesis of [Ga]-MFI

The materials for [Ga]-MFI synthesis were Ludox-AS40 as a silica source (Du Pont Chem. Co.), $Ga(NO_3)_3$ as a Ga source (Aldrich Chem. Co.; 99.9%), NaOH as an alkali and inorganic cation source (Junsei Chem. Co.), and tetrapropylammonium bromide (TPABr) as an organic template (Dongkyung Hwasung Co.).

[Ga]-MFI was synthesized under atmospheric pressure in a 1.5 l Teflon reactor equipped with a condenser and stirrer, and the reactor was heated with an oil bath. The molar composition of the reactants was $100SiO_2$–Ga_2O_3–$11Na_2O$–11TPABr–$3500H_2O$. The synthesis procedures are as follows. First, 640 g of Ludox-AS40, 50.48 g of 50 wt% NaOH solution, and 1116 g of distilled water were mixed in a propylene beaker (I). Then, 1116 g of distilled water, 50.48 g of 50 wt% NaOH solution, and 21.84 g of gallium(III) nitrate hydrate were poured in another propylene beaker (II) and mixed well. Next, the solution of the beaker (II) was slowly poured into the beaker (I) with a vigorous stirring. Finally, 124.8 g of tetrapropylammonium bromide (TPABr) was added to the mixture. The obtained mixture was, then, poured into the reactor mentioned above, and the reaction was carried out at 97 °C under atmospheric pressure with stirring (300 rpm). The flowsheet for the synthesis of [Ga]-MFI is shown in figure 1. ZSM-5 was also synthesized by the same procedure mentioned above to compare with [Ga]-MFI produced.

2.2. Instrumental analysis

In order to investigate the crystallization of [Ga]-MFI, the reaction was stopped after a predetermined reaction time, and the reactor was quenched. Then, the content of the reactor was filtered with a membrane filter of 0.1 μm, and washed with distilled water until the filtrate became neutral. The obtained solids were dried at 100 °C overnight and reserved in a desiccator. The obtained solids were calcined raising temperature at a rate of 5 °C/min to 550 °C with a flow of 50 ml air/min.

The solids were then characterized by XRD (Siemens, D5005), FT-IR (Nicolet, Impact 400), solid state MAS-NMR (Varian, Plus300), XPS (ESCALAB, 220i), XRF (Rigaku, 3270), and DTG/DTA (SETARAM92-16). For

* To whom correspondence should be addressed.

1011-372X/01/0800-0125$19.50/0

XRD analysis, nickel-filtered Cu K_α X-ray beam was used and scanned from 6° to 55° (in 2θ) for 60 min. For FT-IR analysis, wafers were prepared by mixing KBr with samples in a ratio of about 200 : 1, and the analysis was performed in a range of 400–4000 cm^{-1}. Analytical conditions for ^{71}Ga (91.5 MHz) MASS-NMR were as follows: a single pulse was exited at 45° with a zirconia rotor, repeating interval was 1 s, spinning frequency was 6–7 kHz, scanning number was 8000, and chemical shift was measured by comparing with an external standard $Ga(H_2O)_6^{3+}$. Analytical conditions for ^{29}Si (59.6 MHz) MASS-NMR analysis were as follows:

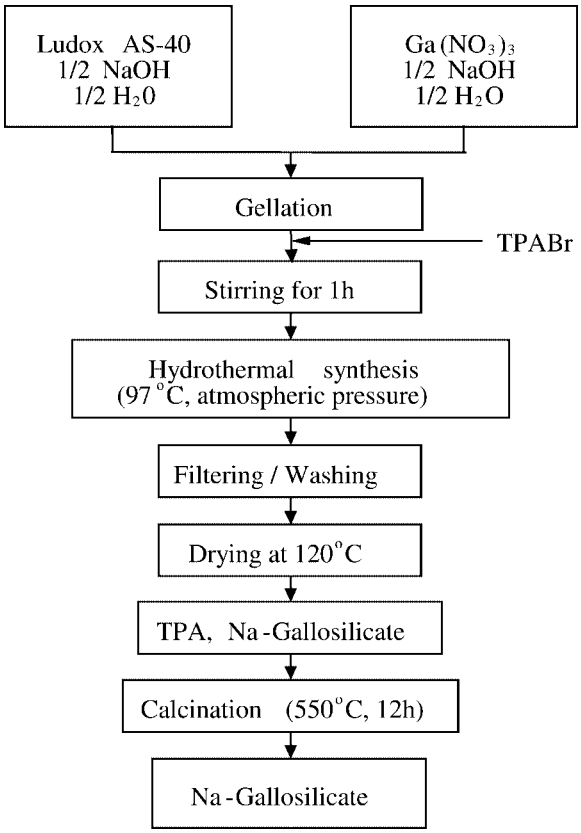

Figure 1. Flowsheet for the synthesis of [Ga]-MFI.

a single pulse was exited at 90° with zirconia rotor, repeating interval was 30 s, spinning frequency was 3.5–4.5 kHz, scanning number was 400, and chemical shift was measured with an external standard TMS (tetramethylsilane). Analytical conditions for ^{13}C (75.5 MHz) MASS-NMR analysis were as follows: a single pulse was exited at 90° with zirconia rotor, repeating interval was 5 s, spinning frequency was 3.5–4.5 kHz, scanning number was 400, and chemical shift was measured with an external standard TMS (tetramethylsilane). XPS analysis was performed with a sample prepared by pressing calcined products into a thin disk of 1 mm thickness. Corrections for charging were made with C 1s peak. For XRF analysis, samples and standard samples were prepared. Na_2CO_3, SiO_2, Ga_2O_3, and Al_2O_3 (all from Johnson Matthey Co., above 99.99% purities) were used to prepare the standard samples and melting agent was anhydrous LiB_4O_7 (Claisse Inc.). DTG/DTA analysis was carried out with a SETRAM92-16. Samples were heated up to 800 °C with a heating rate of 10 °C/min. Ar gas was flowed during the heating and DTA base line was corrected using Al_2O_3 standard.

3. Results and discussion

3.1. Composition change

The composition and physico-chemical properties of the prepared [Ga]-MFI zeolites were characterized using XRF and XPS, and the results are summarized in table 1. Except for the initial gel formation state, the molar ratios of Si to Ga_2 between the surface and the bulk were almost the same. This result reveals that the crystallization of [Ga]-MFI takes place homogeneously, indicating the uniform distribution of Ga throughout the zeolite framework.

In table 1, three XPS peaks of Ga 2p are observed at 1119.7, 1118.9, and 1117.8 eV at the initial state, while only one peak is observed at 1119.2 eV after 72 h of reaction. This result suggests that there were three kinds of Ga species in the initial state but it became one kind after 72 h of reaction. The binding energy of 1119.2 eV of Ga 2p of the final

Table 1
Physico-chemical properties of the synthesized [Ga]-MFI as a function of synthesis time.[a]

Synthesis time	Analysis by XRF (wt%)					Analysis by XPS			
(h)	SiO_2	Ga_2O_3	Na_2O	Mole ratio		Mole ratio	Binding energy[b] (eV)		
				SiO_2/Ga_2O_3	Na_2O/Ga_2O_3	SiO_2/Ga_2O_3	Ga $2p_3$	O 1s	Si 2p
Initial	93.4	2.78	3.58	105.2	3.9	165.4	1119.7 1118.9 1117.8	531.9	103.8
32	94.8	2.86	2.08	103.3	2.2	–	–	–	–
60	94.7	2.95	2.12	100.5	2.2	–	–	–	–
63	94.9	2.88	2.01	102.6	2.1	104.2	1120.4 1119.1	532.7	104
66	94.9	2.91	1.97	102.1	2.0	103.1	1119.2	532.7	104
69	95.4	2.83	1.56	105.3	1.7	–	–	–	–
72	95.3	2.91	1.54	102.5	1.6	102.4	1119.2	532.7	104

[a] Initial mole ratios of the reactants: $SiO_2/Ga_2O_3 = 100$; $SiO_2/Na_2O = 9$; $SiO_2/TPA_2O = 9$; and $H_2O/SiO_2 = 35$.
[b] Referenced to the C 1s of 285 ± 0.2 eV.

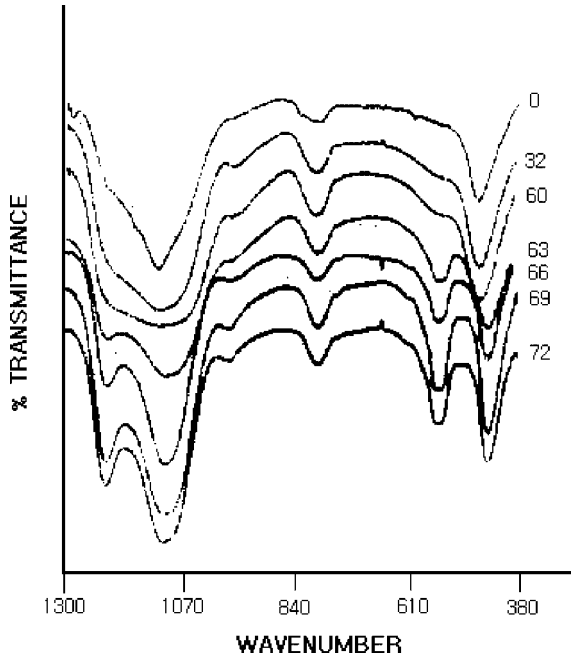

Figure 2. FT-IR spectra for products as a function of synthesis time.

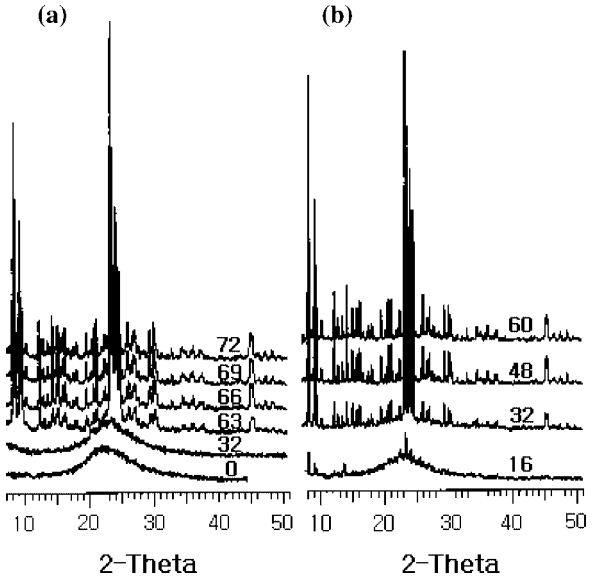

Figure 3. X-ray diffraction patterns for products as a function of synthesis time: (a) [Ga]-MFI and (b) ZSM-5.

product is higher than those of Ga (1117 eV) and Ga_2O_3 (1117.7 eV). This reveals that the gallium existing in the lattice of [Ga]-MFI is GaO_4^- tetrahedral form, so the gallium can have a higher oxidation number [24].

3.2. Structure change during the crystallization

The structure changes of the products with synthesis time were investigated using several analytical instruments. The formation of the unit cell structure of [Ga]-MFI was identified by FT-IR, the crystallinity and phase changes with synthesis time were identified by XRD, the gallium and silicon species existing in [Ga]-MFI framework by ^{71}Ga- and ^{29}Si-MAS-NMR, and the straight- and sinusoidal-type channels that are an unique structure of MFI-type zeolite by ^{13}C-CPMAS-NMR.

3.2.1. FT-IR

Using FT-IR, one can easily identify the five-member ring and double five-member ring of MFI-type zeolite as well as its unit cell structure. The MFI-type zeolites exhibit their unique IR peaks in the regions of 1220 and 550 cm^{-1} [25,26]. The IR spectra of the products with synthesis time are presented in figure 2. Peaks in the regions of 1220 and 550 cm^{-1}, corresponding to the five-member ring and double five-member ring (D5R), were observed after 32 h of reaction, and a new peak around 970 cm^{-1}, which is not observed in ZSM-5 and silicalite, was observed. On and after the synthesis time of 63 h of reaction, the peak for a T–O bonding (attributed by the internal vibration of tetrahedral TO_4) shifted from 475 to 450 cm^{-1}. A similar phenomenon was observed in the XPS result listed in table 1, in which the binding energy of O 1s shifted from 531.9 (initial) to 532.7 eV (after 63 h). As can be seen in figure 2, the peaks for the external linkage vibration of five-member ring and D5R were observed at 1220 and 550 cm^{-1}, respectively, beyond 63 h of reaction. Consequently, it would appear that the shift of the T–O wave number and the change of the binding energy of O 1s stem from a change in the environment of the TO_4, which is caused by the formation of the crystalline structure due to the condensation of SBU (secondary building unit) and chains formed from PBU (primary building unit). It is concluded that the final products are the MFI structure by the unique peaks observed at 454, 547, 794, 1110, and 1220 cm^{-1}.

3.2.2. X-ray diffraction

The phases of the products ([Ga]-MFI) were identified using XRD as a function of the synthesis time. In order to compare the structures of the products with ZSM-5, which has the same structure with [Ga]-MFI, ZSM-5 was also synthesized under the same synthesis condition. The XRD patterns for [Ga]-MFI and ZSM-5 are shown in figure 3. In figure 3, both [Ga]-MFI and ZSM-5 exhibited a typical MFI structure [27,28]. ZSM-5 exhibited typical MFI peaks after 32 h, whereas the [Ga]-MFI exhibited after 63 h.

In figures 4 and 5, the XRD peaks of [Ga]-MFI shifted slightly to a lower angle value (2θ) with the progress of crystallization, indicating a shift to a larger lattice space. This phenomenon may be due to the increase in unit cell parameters by the progress of crystallization.

The crystallinity of ZSM-5 and [Ga]-MFI with synthesis time is shown in figure 6. ZSM-5 shows a typical S-type crystallization curve, whereas [Ga]-MFI does not clearly show the curve. [Ga]-MFI shows a slower nucleation process (namely, a longer nucleation period) followed by a rapid crystal growth, while the ZSM-5 shows a gradual crystallization process. Oh *et al.* [29] reported that one of the key factors in the crystallization of MFI-type zeolites is the action of OH^- ions. Erdem and Sand [30] re-

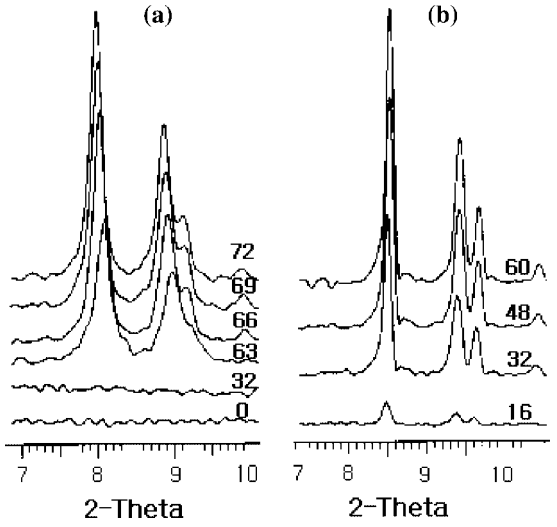

Figure 4. X-ray diffraction patterns for products as a function of synthesis time: (a) [Ga]-MFI and (b) ZSM-5.

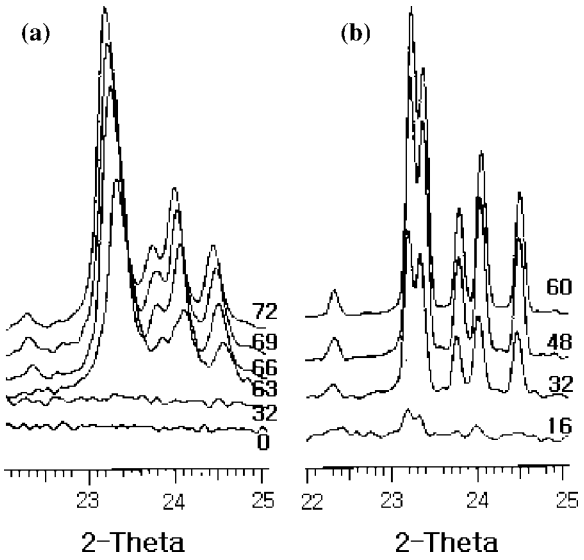

Figure 5. X-ray diffraction patterns for products as a function of synthesis time: (a) [Ga]-MFI and (b) ZSM-5.

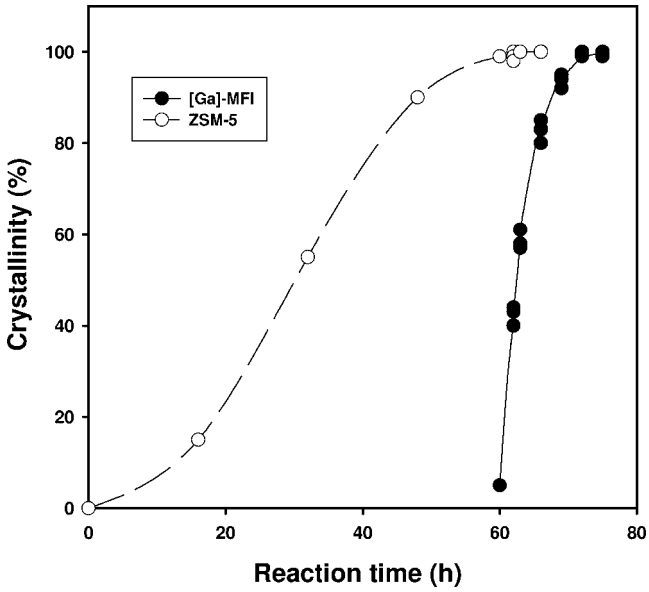

Figure 6. Crystallinity of [Ga]-MFI and ZSM-5 as a function of synthesis time.

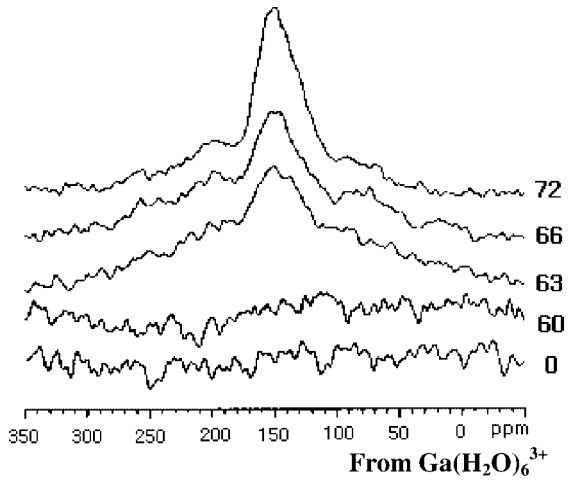

Figure 7. ^{71}Ga-MAS-NMR spectra for products as a function of synthesis time.

ported that the activation energy of the nucleation of ZSM-5 ($Si/Al_2 = 28$) is five times larger than that of the MFI-type silicalite (no aluminum, silicon only). He explained that this phenomenon is caused by the existence of aluminum that lowers the decomposition of the silica gel by consuming OH^- ions of the solution because of its four-coordination numbers ($Al(OH)_4^-$). Therefore, the longer nucleation period of the [Ga]-MFI in this study can be understood with the same reason mentioned above; that is, the gallium, with six-coordination numbers, consumes more OH^- than the aluminum does.

3.2.3. Solid state MAS-NMR

The identification of the existence of a substituted metal in a zeolite framework becomes possible with the use of the solid state MAS-NMR. Figure 7 shows the spectra of ^{71}Ga-MAS-NMR with synthesis time. A single peak around 150 ppm, which corresponds to a chemical shift from $Ga(H_2O)_6^{3+}$, is observed. This is due to a chemical shift of the gallium coordinated tetrahedrally in the zeolite framework [31,32]. The peak becomes larger with synthesis time, indicating the incorporation of gallium into the zeolite. Though gallium species in the initial gel-state were already confirmed by XRF and XPS as summarized in table 1, the peak (observed around 150 ppm) is not observed at the initial state in figure 7. This can be attributed to the fact that the detection of a non-tetrahedral gallium species is difficult because of its disorderliness [32].

The ^{29}Si-MAS-NMR spectra with synthesis time are shown in figure 8. The peaks for the Q^4 [Si(OGa)] structure are observed in a range of −98 to −120 ppm for all the synthesis times. After 63 h, the peaks for Si(OGa) and Si(1Ga) are also observed at −112 and −104 ppm, respectively [33].

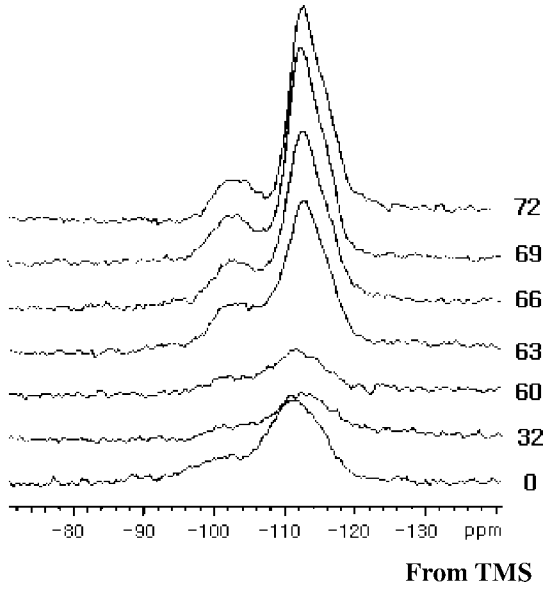

Figure 8. ^{29}Si-MAS-NMR spectra for products as a function of synthesis time.

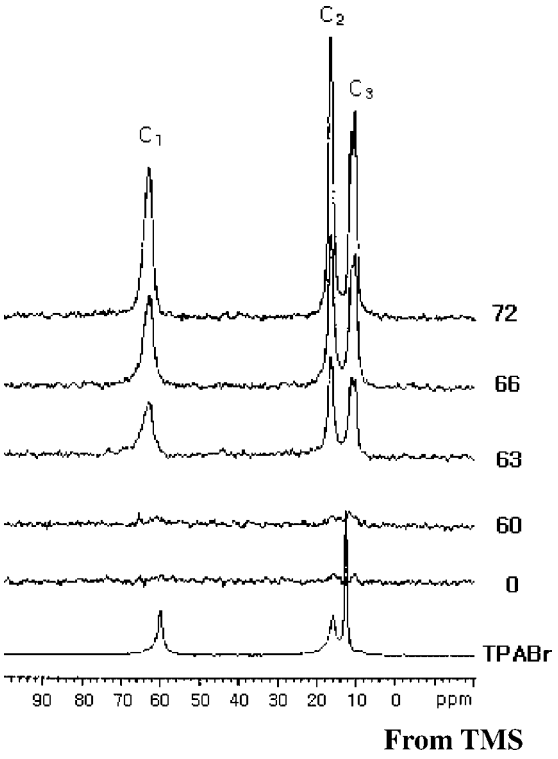

Figure 9. ^{13}C-CPMAS-NMR spectra for products as a function of synthesis time.

The ^{13}C-CPMAS-NMR spectra with synthesis time are presented in figure 9. After 63 h, the peaks for the occluded organic template (TPA^+) are observed and progressively increased with the synthesis time. The intensity of the ^{13}C-CPMAS NMR spectra is well consistent with the crystallinity results of XRD. Therefore, the intensity of the ^{13}C-CPMAS-NMR spectra can be used as a measure of the crystallinity of zeolites [34,35]. The spectra for the occluded organic template are slightly shifted from the original TPABr. It has been known that the differences in the shifted peaks stem from a distortion of the symmetric TPA^+ ion in the porous zeolite structure and/or an interaction of the TPA^+ ion with the zeolite [34].

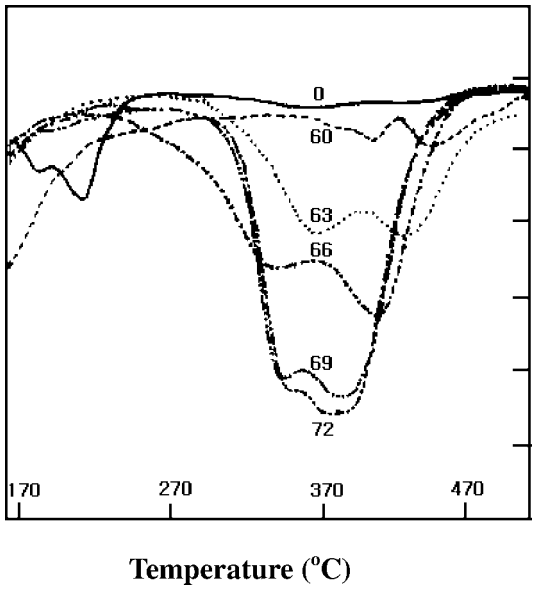

Figure 10. DTG curves for products as a function of synthesis time.

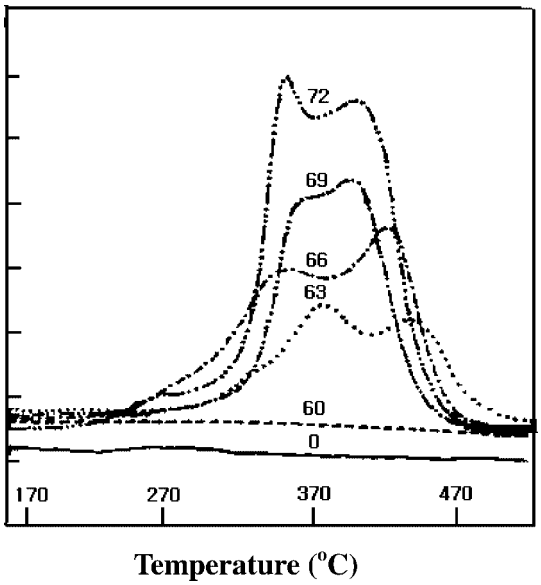

Figure 11. DTA curves for products as a function of synthesis time.

3.2.4. Thermal analysis

Thermal analyses of the products were carried out to get more information in relation to the ^{13}C-CPMAS-NMR. The results are presented in figures 10 and 11. Both the weight loss and the heat evolution due to the removal of the organic template are observed at 280–450 °C in figures 10 and 11, respectively. The DTG and DTA curves clearly show the removal of the organic template after 63 h, and become more significant with the synthesis time, showing good ac-

cordance with the ^{13}C-CPMAS-NMR results. The amount of organic template occluded in the structure was increased with the synthesis time, and the removal temperature of the organic template was lowered with the synthesis time. This phenomenon infers that the interaction between organic template and zeolite lattice becomes weak because of a stabilization of the zeolite structure with time.

4. Conclusion

The [Ga]-MFI was successfully synthesized under atmospheric pressure at 97 °C in 72 h. The final products were verified to be a typical MFI-type zeolite. It was possible to verify the gallium species coordinated in the zeolite framework using ^{71}Ga-MAS-NMR. It was found that the nucleation of [Ga]-MFI took quite a long time, while the crystallization took place very fast. It is supposed that the nucleation is a rate-controlling step in [Ga]-MFI synthesis under atmospheric pressure. Therefore, if the induction period of nucleation can be shortened, it would be possible to synthesize [Ga]-MFI commercially under atmospheric pressure.

Acknowledgement

This work was supported by Brain Korea 21 project.

References

[1] M. Guisnet, N.S. Gnep and F. Alario, Appl. Catal. 89 (1992) 1.
[2] G. Giannetto, A. Montes, N.S. Gnep, A. Florentino, P. Cartraud and M. Guisnet, J. Catal. 145 (1993) 86.
[3] V.R. Choudhary, A.K. Kinage and M. Guisnet, J. Catal. 158 (1996) 537.
[4] W.G. Kim, J.H. Kim, B.J. Ahn and G. Seo, Korean J. Chem. Eng. 18 (2001) 120.
[5] N.S. Gnep, J.Y. Doyemet and M. Guisnet, Stud. Surf. Sci. Catal. 46 (1989) 153.
[6] A.Y. Khodakov, L.M. Kustov, T.N. Bondarenko, A. Dergachev, V.B. Kazansky, K.M. Minachev, G. Borbely and H.K. Beyer, Zeolites 10 (1990) 603.
[7] C.R. Bayense, A.J.H.P. van der Pol and J.H.C. van Hoff, Appl. Catal. 72 (1991) 81.
[8] P. Meriaudeau and C. Naccache, J. Mol. Catal. 59 (1990) L31.
[9] N.S. Gnep, J. Mol. Catal. 45 (1998) 281.
[10] V.I. Yakerson, T.V. Vasina, L.I. Lafer, V.P. Sytnyk, G.L. Dylch and A.V. Mokhov, Catal. Lett. 3 (1989) 339.
[11] L.M. Thomas and X. Liu, J. Phys. Chem. 90 (1986) 4843.
[12] V.R. Choudhary, P. Devadas, A.K. Kinage, C. Sivadinarayana and M. Guisnet, J. Catal. 158 (1996) 23.
[13] D.K. Simmons, R. Szostok, P.K. Agrawal and T.L. Thomas, J. Catal. 106 (1987) 287.
[14] T. Inui, Y. Makino, F. Okazumi, S. Nagano and A. Miyamoto, Ind. Eng. Chem. Res. 26 (1987) 647.
[15] J. Kanai and N. Kawata, Appl. Catal. 55 (1989) 115.
[16] Mobil Oil Corp., EP187496 (1986).
[17] Mobil Oil Corp., EP327189 (1989).
[18] Mitsubishi Chem. Corp., JP09020706 (1997).
[19] Chiyoda Corp., JP05269385 (1993).
[20] Vaw ver Aluminium Werke Ag., DE4021118 (1992).
[21] G. Giannetto, R. Monque, J. Perez and L. Garcia, Zeolites 13 (1993) 557.
[22] V.R. Choudhary, A.K. Kinage, C. Sivadinarayana, P. Devadas, S.D. Sansare and M. Guisnet, J. Catal. 158 (1996) 34.
[23] V.R. Choudhary and A.K. Kinage, Zeolites 18 (1997) 274.
[24] E.S. Shpiro, D.P. Shevchenko, O.P. Tkachenko and R.V. Dmitriev, Appl. Catal. A 107 (1994) 147.
[25] R. Szostak, *Molecular Sieve – Principles of Synthesis and Identification* (1989) p. 197.
[26] M.A. Camblor, Zeolites 12 (1992) 280.
[27] R.J. Argauer and G.R. Landolt, US Patent 3 702 886 (1972).
[28] G. Gianetto, R. Monque, J. Perez, J. Papa and L. Garcia, Zeolites 13 (1993) 559.
[29] H.S. Oh, K.K. Kang, M.H. Kim and H.K. Rhee, Korean J. Chem. Eng. 18 (2001) 113.
[30] A. Erdem and L.B. Sand, J. Catal. 60 (1979) 241.
[31] H.C.K. Timken and E. Oldfield, J. Am. Chem. Soc. 109 (1987) 7669.
[32] C.R. Bayense, J.H.C. Van Hooff, A.P.M. Kentquens, J.W. DeHaan and L.J.M. Van de Ven, in: *Proc. 8th Int. Zeolite Conference* (1989) p. 105.
[33] X.S. Lin and J. Klinowski, J. Phys. Chem. 96 (1992) 3403.
[34] Z. Gabelica, J.B. Nagy and G. Debras, J. Catal. 84 (1983) 256.
[35] J.B. Nagy, P. Bodart, E.G. Derouane, Z. Gebelica and A. Nastro, in: *Proc. 7th Int. Zeolite Conference* (1986) p. 231.
[36] G. Giannetto, R. Monque, J. Perez and L. Garcia, Zeolites 13 (1993) 557.
[37] L. Brabec, M. Jeschke, R. Klik, J. Novakova, L. Kubelkova and D. Freude, Appl. Catal. A 167 (1998) 309.